Excitation of Kinetic Geodesic Acoustic Modes by Drift Waves in Nonuniform Plasmas

Z. Qiu[1], L. Chen[1,2] and F. Zonca[1,3]

[1] *Inst. Fusion Theory and Simulation, Zhejiang Univ., Hangzhou 310027, P.R.C.*

[2] *Dept. Physics and Astronomy, Univ. of California, Irvine CA 92697-4575, U.S.A.*

[3] *Associazione Euratom-ENEA sulla Fusione, C.P. 65 - I-00044 - Frascati, Italy*

Effects of system nonuniformities and kinetic dispersiveness on the spontaneous excitation of Geodesic Acoustic Mode (GAM) by Drift Wave (DW) turbulence are investigated based on nonlinear gyrokinetic theory. The coupled nonlinear equations describing parametric decay of DW into GAM and DW lower sideband are derived, and then solved both analytically and numerically to investigate the effects on the parametric decay process due to system nonuniformities; such as nonuniform diamagnetic frequency, finite radial envelope of DW pump, and kinetic dispersiveness. It is found that, the parametric decay process is a convective instability for typical tokamak parameters when finite group velocities of DW and GAM associated with kinetic dispersiveness and finite radial envelope are taken into account. When, however, nonuniformity of diamagnetic frequency is taken into account, the parametric decay process becomes, time asymptotically, a quasi-exponentially growing absolute instability. This result is possibly that in the present work of most significant practical impact for DW induced turbulence transport.

I. INTRODUCTION

Drift wave (DW) type turbulence [1] induced by expansion free energy due to plasma nonuniformities is generally considered to be the primary cause of anomalous transport in tokamak plasmas; and the resultant transport fluxes, typically, scale linearly with the turbulence intensity [2]. It has been demonstrated, by both analytical theory and large scale simulations, that the $n = 0$ zonal flow (ZF), including both the low-frequency ZF (LFZF) [3–5] and its finite frequency counterpart, the geodesic acoustic mode (GAM) [6, 7],

can be spontaneously driven by DW turbulence and plays important role in its regulation by scattering it into stable short radial wavelength fluctuations [8, 9]. Thus, excitation of ZF, which provides a possible mechanism for DW turbulence self-regulation, is considered to be crucial in triggering L-H transition and has received major attention in fusion research in the past decade.

GAM is predominantly an electrostatic mode unique to toroidal plasmas, characterized by an $n = 0/m = 0$ scalar potential, and an $n = 0/m = 1$ up-down antisymmetric density perturbation. Here, n/m are the toroidal/poloidal mode numbers. Similar to LFZF, strong coherent interactions between GAM and DW turbulences are also identified experimentally. Observations generally show an inverse relation between GAM intensity and background turbulence level. Resonant coherent parametric decay process [10, 11] is proposed as the mechanism for GAM excitation by DW turbulence, during which DW turbulence decay into a short radial wavelength lower sideband and a GAM with the constraint of frequency and wavenumber matching conditions [7, 9].

The excitation of GAM by DW turbulence has been investigated using the paradigm of parametric decay instability in several earlier works [12–19]. However, in these works, the excitation of GAM is investigated either ignoring the plasma nonuniformities or the contribution of kinetic dispersiveness. As we will show in this work, plasma nonuniformities, such as the nonuniformity of diamagnetic frequency $\omega_*(r)$ and/or GAM continuum, and the finite linear group velocities of GAM and DW sideband, due to the kinetic dispersiveness, play important roles in the excitation of GAM and qualitatively change the features of parametric decay instability. Thus, the effects of kinetic dispersiveness and plasma nonuniformities must be properly taken into account to correctly assess the nonlinear excitation of GAM and the size scaling of transport in a realistic experiment [20].

There are three different spatial scales in GAM-DW nonlinear interactions; i.e., the scale length of the DW radial envelope L_P, the scale length of diamagnetic frequency nonuniformity L_*, and the scale length of GAM continuum L_G. Here, $|L_P| \sim \sqrt{\rho_i L_*} \ll |L_*| \sim |L_G| \sim a$, with a being the minor radius of the tokamak. Due to the scale separation, effects of nonuniform $\omega_*(r)$ and $\omega_G(r)$ can be ignored when one considers implications of finite group velocities and finite pump scale length, L_P, on GAM excitation. Meanwhile, we note that earlier local theories are, thus, valid only when one considers radial scale lengths shorter than L_P. In this paper, we will investigate the effects of finite L_P, L_* and L_G on GAM excitation.

The rest of the paper is organized as follows. Section II presents the physical model and derivation of the governing equation using a nonlinear gyrokinetic approach. In Sec. III, effects of finite kinetic dispersiveness and finite pump wave scale length on GAM excitation are investigated. We show that, when finite group velocities associated with kinetic dispersiveness are considered, GAM excitation is a convective instability for typical tokamak parameters; which is, thus, of less interest for confinement research. Section IV considers the consequences of diamagnetic frequency and GAM continuum nonuniformities on the parametric instability. Section IV A, in particular, considers effects of nonuniform diamagnetic frequency on GAM excitation, while assuming uniform pump and uniform GAM frequency. On a longer time scale, the excitation of GAM becomes a quasi-exponentially growing absolute instability due to the trapping of DW sideband and formation of eigenmode between turning points induced by nonuniform diamagnetic frequency. Finally, in Sec. IV B, the parametric instability is considered taking all three nonuniformities self-consistently. Summary and discussions on possible extensions of this work are given in Sec. V

II. THE PHYSICAL MODEL

The derivation of the coupled nonlinear DW-GAM equations follow closely Refs. 7, 9 and 21. Here, we assume that the DW and GAM are both electrostatic perturbations. Furthermore, we assume sufficient proximity to the marginal stability with $|\gamma_L/\omega| \ll 1$, such that GAM will only modify the radial envelope of DWs, while the parallel mode structure of DW is not affected. The nonlinear dynamic evolution of the coupled DW and GAM system is described in terms of a three-wave parametric decay instability; i.e., each fluctuation is taken to be coherent and composed of a single $n \neq 0$ DW, $\delta\phi_d$, and a GAM $\delta\phi_G$. The DW is taken to consist of a pump wave $(\omega_P, \mathbf{k}_P)$ and a lower sideband $(\omega_S, \mathbf{k}_S)$ due to the nonlinear interactions of the pump with GAM (ω_G, k_G). Thus,

$$\begin{aligned}
\delta\phi_d &= \delta\phi_P + \delta\phi_S, \\
\delta\phi_P &= A_P e^{-in\xi - i\omega_P t} \sum_m e^{im\theta} \Phi_0(nq - m) + c.c., \\
\delta\phi_S &= A_S e^{in\xi - i(\omega_G - \omega_P)t} \sum_m e^{-im\theta} \Phi_0^*(nq - m) + c.c., \\
\delta\phi_G &= A_G e^{-i\omega_G t} + c.c.;
\end{aligned}$$

and the eikonal Ansatz is assumed for the radial envelopes; i.e.,

$$\begin{aligned} A_P &= e^{i\int k_P dr}, \\ A_S &= e^{-i\int k_P dr}\left(e^{i\int k_G dr} + c.c.\right), \\ A_G &= e^{i\int k_G dr} + c.c.. \end{aligned}$$

The subscripts d, P, S and G represent, respectively, drift wave, pump, sideband, and GAM. $\phi_0(nq-m)$ is the short radial scale structure associated with finite $k_\parallel$ and magnetic shear

$$\Phi_0(nq-m) \equiv \frac{1}{\sqrt{2\pi}}\int_{-\infty}^{\infty} e^{-i(nq-m)\eta}\psi_o(\eta)d\eta,$$

with η being the extended coordinate along the magnetic filed $\mathbf{B}$. $\Psi_0(\eta)$, thus, corresponds to parallel mode structure, and the normalization $\int_{-\infty}^{\infty}|\psi_0(\eta)|^2 d\eta = 1$ is assumed. The other notations are standard. We note here that, for simplicity, the $m \neq 0$ poloidal sidebands of GAM scalar potential are ignored. Extension of the following analysis to include $\delta\phi_G$ poloidal sidebands associated with finite T_e/T_i is tedious but straightforward.

The nonlinear response can be systematically derived from the nonlinear gyrokinetic equation [22]

$$\begin{aligned} \left(\partial_t + \omega_{tr}\partial_\theta + i\omega_d\right)_k \delta H_k = &- \frac{q_s}{m} J_k \left(\partial_t \delta\phi \partial_E + \frac{\nabla_X \delta\phi \times \hat{\mathbf{b}}}{\Omega_c}\cdot\nabla_X\right) F_0 \\ &+ \frac{q_s}{m}\sum_{\mathbf{k}=\mathbf{k}'+\mathbf{k}''} J_{k'}\frac{\nabla_X\delta\phi_{k'}\times\hat{\mathbf{b}}}{\Omega_c}\cdot\nabla_X\delta H_{k''}; \end{aligned} \tag{1}$$

where δH is the nonadiabatic part of the fluctuating particle distribution function, and

$$\delta F = \frac{q_s}{m}\delta\phi\frac{\partial}{\partial E}F_0 + \sum_{\mathbf{k}_\perp}\exp(-i\mathbf{k}_\perp\cdot\mathbf{v}\times\mathbf{b}/\Omega_c)\delta H_k.$$

Note that here, for notation brevity, the subscript s for particle species (e and i for electrons and ions, respectively) is kept only in the particle charge q_s. Furthermore, a large aspect-ratio axisymmetric tokamak with equilibrium magnetic field given by $\mathbf{B}_0 = B_0(\mathbf{e}_\xi/(1+\epsilon\cos\theta) + (\epsilon/q)\mathbf{e}_\theta)$ is considered in this work. Here, ξ and θ are, respectively, toroidal and poloidal angles of the torus, $\epsilon = r/R_0 \ll 1$ is the inverse aspect ratio, r and R_0 are the minor and major radii, and (r,θ,ξ) are straight-field-line toroidal flux coordinates. Meanwhile, $\omega_{tr} = v_\parallel/qR_0$ is the transit frequency, ω_d is the magnetic drift frequency, $k_\perp$ is the perpendicular wave vector, $\rho_L = mcv_\perp/q_sB$ is the Larmor radius, $\Omega = q_sB/mc$ is the gyrofrequency, q is

the tokamak safety factor, $J_k = J_0(k_\perp \rho_L)$ is the Bessel function accounting for finite Larmor radius (FLR) effects, and $E = (v_\parallel^2 + v_\perp^2)/2$.

The nonlinear equations for the GAM-DW system can be derived in terms of the quasineutrality conditions

$$\frac{n_0 e^2}{T_i}\left(1+\frac{T_i}{T_e}\right)\delta\phi_k = \langle eJ_k\delta H_i\rangle_k - \langle e\delta H_e\rangle_k; \tag{2}$$

where, subscript "k" stands for P, S or G and angular brackets indicate velocity space integration. By separating the linear from nonlinear response as $\delta H \equiv \delta H^L + \delta H^{NL}$, and applying the $\omega \gg \omega_{tr,i}, \omega_{d,i}$ assumptions for the nonlinear ion responses, we obtain, after straightforward algebra,

$$\begin{aligned}
&\frac{n_0 e^2}{T_i}\left(1+\frac{T_i}{T_e}\right)\delta\phi_k - \langle eJ_k\delta H_i^L\rangle_k + \langle e\delta H_e^L\rangle \\
=\ & -\frac{i}{\omega_k}\left\langle e\frac{c}{B}\sum_{\mathbf{k}=\mathbf{k}'+\mathbf{k}''}\mathbf{b}\cdot(\mathbf{k}''\times\mathbf{k}')\delta\phi_{k'}\delta H_{e,k''}\right\rangle_k - \langle e\delta H_e^{NL}\rangle_k \\
& -\frac{i}{\omega_k}\left\langle e\frac{c}{B}\sum_{\mathbf{k}=\mathbf{k}'+\mathbf{k}''}\mathbf{b}\cdot(\mathbf{k}''_\perp\times\mathbf{k}'_\perp)\left(J_kJ_{k'}-J_{k''}\right)\delta\phi_{k'}\delta H_{i,k''}\right\rangle_k .
\end{aligned} \tag{3}$$

For the $n \neq 0$ DW, the electron response is adiabatic due to the fast electron motion along the magnetic field line shielding parallel electric field; thus, $\delta H_{e,d} = 0$. While for GAM, with $n = m = 0$, the nonadiabatic electron response can be solved from electron gyrokinetic equation as in [23], and we obtain

$$\delta H_{e,G}^L \ = \ -\frac{e}{T_e}\delta\phi_G F_0,$$

and

$$\delta H_{e,G}^{NL} \ = \ 0.$$

For nonlinear DW equation, with typically $k_\perp\rho_i \ll 1$, the first term on the right hand side of equation (3) dominates; since $\delta H_{e,d} = 0$ and $\delta H_{e,G} \neq 0$ such that there is no commutative cancelation. The last term on the right hand side of equation (3) is formally $O(k_r^2\rho_i^2)$ smaller than the first term. The nonlinear DW equation, then reduces to

$$\frac{n_0 e^2}{T_i}\left(1+\frac{T_i}{T_e}\right)\delta\phi_k - \langle eJ_k\delta H_i^L\rangle_k = e\frac{c}{B}\frac{1}{\omega_k}k'_\theta\delta\phi_{k'}\frac{\partial\langle\delta H_{e,G}\rangle}{\partial r}, \tag{4}$$

with the constraint $\mathbf{k} = \mathbf{k}' + \mathbf{k}_G$.

For GAM, the first two terms on the right hand side of equation (3) are both zero. The nonlinear GAM equation can be written as

$$\begin{aligned}
&\frac{n_0e^2}{T_i}\left(1+\frac{T_i}{T_e}\right)\delta\phi_G-\left\langle eJ_G\delta H^L_{i,G}\right\rangle+\left\langle e\delta H^L_{e,G}\right\rangle\\
=&-\frac{i}{\omega_G}\left\langle e\frac{c}{B}\mathbf{b}\cdot\mathbf{k}''\times\mathbf{k}'\left(J_{k'}-J_{k''}\right)\left(\delta\phi_{k'}\delta H_{k''}+\delta\phi_{k'}\delta H_{k''}\right)\right\rangle_k\\
&-\frac{i}{\omega_G}\left\langle e\frac{c}{B}\mathbf{b}\cdot\mathbf{k}''\times\mathbf{k}'\left(J_k-1\right)\left(J_{k'}\delta\phi_{k'}\delta H_{k''}-J_{k''}\delta\phi_{k''}\delta H_{k'}\right)\right\rangle_k. \qquad (5)
\end{aligned}$$

For DW turbulence, $|\omega|\simeq|\omega_*|\gg|\omega_{tr}|,|\omega_d|$, so that the second term on the right hand side of equation (5) is $O(\omega_{tr}^2/\omega^2)$ or $O(\omega_d^2/\omega^2)$ smaller than the first term. The dominant nonlinear term, the first term, is of the form of the well-known Reynolds stress.

The nonlinear coupled DW-GAM equations can be obtained from equations (4) and (5). Here we assume that the amplitudes of the two daughter waves, i.e., GAM and DW lower sideband, are much smaller than the pump wave; and derive the nonlinear equations describing GAM and DW sideband excitation. The DW sideband equation can be written as

$$D_S\partial_tA_S=-\frac{c}{B}k_{\theta,P}k_{r,G}\frac{T_i}{T_e}A^*_PA_G, \qquad (6)$$

with $D_S\equiv D_0(\omega_S,\mathbf{k}_S,r)$, and D_0 is the linear dispersion function of DW formally defined by

$$D_0\equiv1+\frac{T_i}{T_e}-\int_{-\infty}^{\infty}\psi_0(\eta)\left\langle eJ_0(\gamma)\delta H^L_i\right\rangle d\eta/\left(\frac{n_0e^2}{T_i}A_P\right).$$

The nonlinear GAM equation, on the other hand, can be written as

$$\epsilon_G\partial_t\delta\phi_G=-\alpha_i\frac{c}{2B}k_{\theta,P}k^3_{r,G}\rho_i^2\delta\phi_S\delta\phi_P, \qquad (7)$$

with the linear dispersion function of GAM, ϵ_G, formally given by [7]

$$\epsilon_G\equiv\left[\frac{n_0e^2}{T_i}\left(1+\frac{T_i}{T_e}\right)\delta\phi_G-\left\langle eJ_G\delta H^L_{i,G}\right\rangle+\left\langle e\delta H^L_{e,G}\right\rangle\right]\Big/\left(\frac{n_0e^2}{T_i}\delta\phi_G\right),$$

and the coefficient $\alpha_i=1+\delta P_\perp/(en_0\delta\phi_P)$ in the $|k_\perp\rho_i|<1$ limit [9].

Since the DW sideband has a frequency and wavenumber very close to the pump wave $\delta\phi_{P^*}$ due to the frequency separations $|\omega_G|\ll|\omega_P|$, $D_S(\omega_S,\mathbf{k}_S,r)$ can be expanded about ω_{P*} and $\mathbf{k}_{P*}$ to yield

$$\begin{aligned}
D_S(\omega_S,\mathbf{k}_S,r)=&\ D_{0r}(\omega_{P^*},k_{P^*},r_0)+\frac{\partial D_{0r}}{\partial\omega_{P^*}}(i\partial_t+\omega_G)+\left.\frac{\partial D_{0r}}{\partial k_S}\right|_0k_S+\frac{1}{2}\left.\frac{\partial^2D_{0r}}{\partial k_S^2}\right|_0k_G^2\\
&+\frac{\partial D_{0r}}{\partial r_0}(r-r_0)+\frac{1}{2}\frac{\partial^2D_{0r}}{\partial r_0^2}(r-r_0)^2+iD_I+\cdots.
\end{aligned}$$

Noting that drift waves have, typically, quadratic dispersiveness, D_0 may then be modeled as

$$D_0 = \omega - \omega_* \exp(-(r-r_0)^2/L_*^2) + C_d \omega_* \rho_i^2 k_i^2 + iD_I,$$

assuming a Gaussian profile for ω_*. We then have

$$D_S = i\left(\partial_t + \gamma_S + i\omega_P - i\omega_*\left(1 - \frac{(r-r_0)^2}{L_*^2}\right) - iC_d\omega_*\rho_i^2\frac{\partial^2}{\partial r^2}\right), \tag{8}$$

where γ_S represents collisionless damping for DW sideband, and the term proportional to C_d comes from finite radial envelope variation due to the coupling between neighboring poloidal harmonics.

Defining $\mathscr{E} = \partial_r \delta\phi_G/\alpha$, with $\alpha = i(\alpha_i \omega_P T_e/T_i)^{1/2}$, we obtain the following coupled nonlinear equations [24]:

$$\left(\partial_t + \gamma_S + i\omega_P - i\omega_*\left(1 - \frac{(r-r_0)^2}{L_*^2}\right) - iC_d\omega_*\rho_i^2\frac{\partial^2}{\partial r^2}\right) A_S \;=\; \Gamma_0^* \mathscr{E}, \tag{9}$$

$$\left(\partial_t(\partial_t + 2\gamma_G) + \omega_G^2(r) - C_G\omega_G^2(r_0)\rho_i^2\frac{\partial^2}{\partial r^2}\right)\mathscr{E} \;=\; -\Gamma_0 \partial_t \partial_r^2 A_S, \tag{10}$$

in which, $\Gamma_0 \equiv (\alpha_i T_i/\omega_P T_e)^{1/2} c k_{\theta,P}\delta\phi_P/B$ is the normalized pump amplitude. These two equations, equations (9) and (10), describe the parametric decay of the pump DW into a DW lower sideband and a GAM. In this work, we will study the linear parametric excitation of GAM by DW turbulence; emphasizing the effects of nonuniformities due to, e.g., pump finite spatial extent and nonuniform DW frequency, while neglecting the feedback of GAM and DW sideband on DW pump. The feedback of GAM and DW sideband to DW pump is important when their amplitudes become finite. Self-consistent nonlinear investigation of GAM and DW sideband feedbacks on DW pump will be carried out in a future publication.

III. UNIFORM PLASMA: CONVECTIVE GAM AMPLIFICATION

First, we investigate effects of finite group velocities due to kinetic dispersiveness on the parametric excitation of GAM. For simplicity of discussion, only the finite spatial extent of the DW pump, L_P, is taken into account here; while assuming $L_* = L_G = \infty$. Note that, L_P is the radial scale length of the linear DW eigenmode, which is determined by L_* and finite dispersiveness associated with FLR; and one typically has $L_P \propto \sqrt{L_*\rho_i} \ll L_*$. So

the simplification of neglecting the finite pump radial extent is valid when one considers the time scale shorter than L_P/v_G^{NL}, with v_G^{NL} being the nonlinear group velocity [16, 25], which will be determined later.

If two temporal- and spatial-scale expansion of A_S and $\mathscr{E}$ is applied, such that $\partial_t = -i\omega + \partial_\tau$ and $\partial_r = -ik_r + \partial_z$, with $|\partial_\tau| \ll |\omega|$ and $|\partial_z| \ll |k_r|$, the coupled DW sideband and GAM nonlinear equations can be reduced to

$$(\partial_\tau + \gamma_S + V_S\partial_z)A_S = \Gamma_0^*(z)\mathscr{E}, \tag{11}$$

$$(\partial_\tau + \gamma_G + V_G\partial_z)\mathscr{E} = k_r^2\Gamma_0(z)A_S. \tag{12}$$

Here, $V_S = C_d\omega_*\rho_i^2k_r$ and $V_G = C_G\omega_G^2(0)\rho_i^2k_r/\omega$ are, respectively, the linear group velocities of DW sideband and GAM, and ω and k_r are determined from the following frequency and wavenumber matching conditions for resonant decay [7]:

$$\omega - \omega_P + \omega_* - C_d\omega_*\rho_i^2k_r^2 = 0,$$
$$\omega^2 - \omega_G^2 - C_G\omega_G^2(0)\rho_i^2k_r^2 = 0.$$

Equations (11) and (12) recover the results of [7] if the finite linear group velocities are ignored;

$$(\gamma + \gamma_S)(\gamma + \gamma_G) = k_r^2\Gamma_0^2.$$

Thus, parametric excitation by DW favors short wavelength kinetic GAM (KGAM), and the threshold condition for spontaneous excitation can be estimated from $k_r^2\Gamma_0^2 = \gamma_S\gamma_G$ [7]. This also motivates our investigation of the effect of kinetic dispersiveness on KGAM excitation, as it increases with k_r.

When finite group velocities are taken into account, equations (11) and (12) are in the standard form of parametric instability discussed in [26]. From the results of [26], we readily know that the instability is convective for $V_dV_G \propto C_dC_G > 0$; i.e., the DW sideband and GAM linearly propagate in the same direction while being parametrically amplified. For $V_dV_G < 0$, the parametric instability is an absolute instability. To show this more in detail, equations (11) and (12) can be solved both analytically, using an asymptotic approach, and numerically as illustrated in the following.

To investigate the spatiotemporal evolution of the coupled GAM-DW system, let's further simplify the problem, and ignore the spatial dependence of the pump amplitude $\Gamma_0(z)$, i.e.,

we focus on the convective nature of the parametric instability. Taking $\xi = z - V_c t$ with $V_c = (V_d + V_G)/2$, the coupled DW-GAM equations reduce to

$$(\partial_t^2 - V_0^2 \partial_\xi^2)\mathscr{E} = k_r^2 \Gamma_0^2 \mathscr{E} \tag{13}$$

in the wave moving frame, with $V_0 = (V_d - V_G)/2$. If the kinetic dispersiveness is taken as small correction to the temporal growing wave, i.e., $\mathscr{E} = f(\epsilon t, z)\exp(k_r\Gamma_0 t)$, with $|\partial_t \ln(f)| \ll k_r\Gamma_0$, the above equation can be solved, yielding the following asymptotic solution [24]:

$$\mathscr{E} = \frac{C}{\sqrt{t}} \exp\left[k_r\Gamma_0 t - \frac{k_r\Gamma_0}{2V_0^2 t}(z - V_c t)^2\right]. \tag{14}$$

Here, C is a constant coefficient, and the above aysmptotic solution is valid for $|V_0 t| \gg |z - V_c t|$. From this asymptotic solution, we can see that when $V_G V_d > 0$, the coupled DW sideband-GAM wave packet propagates at a hybrid group velocity $V_c = (V_G + V_d)/2$, which is typically much larger than the linear group velocity of GAM by $O(\omega_*/\omega_G)$. This may explain the much larger "nonlinear group velocity" observed in simulation [15, 16] and, also, in experiments [25]; which can not be interpreted in terms of the linear group velocity of KGAM.

In addition to analytic solutions, we have also carried out numerical solution of equations (9) and (10), and the results are shown in Fig. 1. Here, the pump wave amplitude is taken to be Gaussian, and the nonuniformities of ω_* and ω_G are ignored. $C_d = 1$ is fixed, and the sign of C_G can be changed to change the absolute/convective property of the parametric instability. We can see that, for $C_G = 1$, the DW and GAM sideband are coupled together and propagate out of the unstable region. The mode amplitudes at the origin will first grow, then decay; showing the typical features of convective instability. Meanwhile, for $C_G = -1$, the mode amplitudes at the origin will keep growing; demonstrating the characteristics of an absolute instability.

The absolute/convective property of the parametric instability is determined by the sign of $V_G V_d$, and finally, $C_d C_G$. Note C_d is usually positive while C_G is positive for typical tokamak parameters, such as temperature ratio T_e/T_i and/or the tokamak safety factor q. Readers interested in the dependence of the sign of C_G on plasma parameters may refer to [7] for a detailed discussion. Thus, for typical tokamak parameters, the parametric decay of DW pump into GAM and a stable short radial wavelength DW sideband is usually a convective instability. Typically, the generated DW sideband and GAM are coupled together

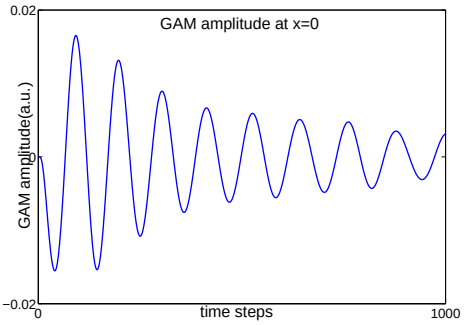

(a) GAM amplitude at $x = 0$. $C_G = 1$

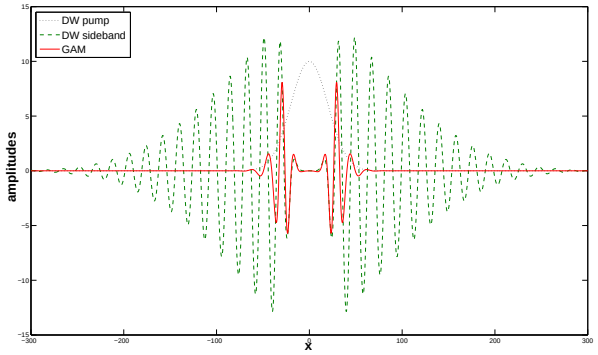

(b) Snapshot of modestructure. $C_G = 1$

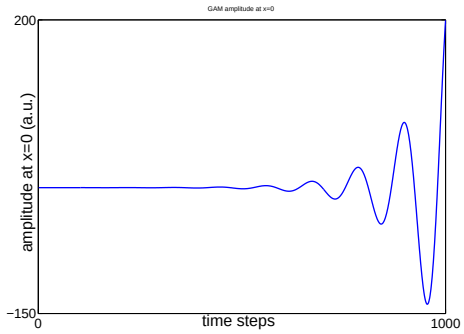

(c) GAM amplitude at $x = 0$. $C_G = -1$

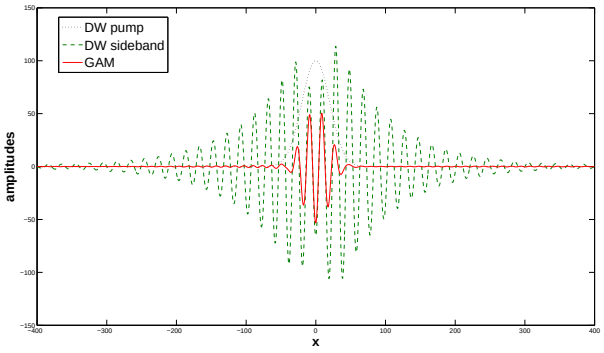

(d) Snapshot of modestructure. $C_G = -1$

FIG. 1: Figs. 1a and 1c are respectively the GAM amplitude at r_0 v.s. time for $C_G = \pm 1$. Figs. 1b and 1d are respectively the snapshot of mode structure at $t = 100/\omega_G$ for $C_G = \pm 1$.

and propagate out of the pump DW localization domain before they can grow to sufficiently large amplitude. Thus, this process is of lesser interest for fusion confinement research, since GAM can not attain a sufficient amplitude to suppress DW turbulence.

IV. NONUNIFORM PLASMA: GAM ABSOLUTE INSTABILITY

A. Nonuniform Diamagnetic Frequency Effect

For typical tokamak parameters, when short spatial scales are considered ($|r - r_0| \leq L_P$) and nonuniformity of $\omega_*(r)$ and/or $\omega_G(r)$ is ignored, the excitation of GAM by DW

turbulence is a convective instability, which is of lesser interest from the confinement point of view. Thus, in order to understand potential important roles of nonlinear DW-GAM dynamics, one needs to consider the nonuniformties of $\omega_*(r)$ and/or $\omega_G(r)$. In this section, we will ignore nonuniformities of both GAM frequency and pump amplitude in order to delineate the effects of nonuniform diamagnetic frequency on GAM excitation. For the simplicity of discussion, collisionless damping of both GAM and DW sideband is also ignored ; i.e., $\gamma_S = \gamma_G = 0$.

Taking $\partial_t = -i\omega$, the coupled nonlinear GAM-DW sideband equations become:

$$\left(\omega - \omega_P + \omega_* \left(1 - \frac{(r-r_0)^2}{L_*^2}\right) + C_d \omega_* \rho_i^2 \frac{\partial^2}{\partial r^2}\right) A_S = i\Gamma_0^* \mathscr{E},$$

$$\left(\omega^2 - \omega_G^2 + C_G \omega_G^2 \rho_i^2 \frac{\partial^2}{\partial r^2}\right) \mathscr{E} = -i\omega\Gamma_0 \frac{\partial^2 A_S}{\partial r^2}.$$

The coupled equations can be solved in Fourier space, and we obtain the nonlinear DW sideband eigenmode equation in k_r space [27]

$$\left(\frac{\omega_*}{L_*^2}\frac{\partial^2}{\partial k_r^2} + \omega - \omega_P + \omega_* - C_d \omega_* \rho_i^2 k_r^2 + \frac{\omega k_r^2 \Gamma_0^2}{\omega^2 - \omega_G^2 - C_G \omega_G^2 \rho_i^2 k_r^2}\right) A_S = 0. \tag{15}$$

Linear DW eigenmode equation in k_r space can be recovered if one ignores the nonlinear term (the term proportional to Γ_0^2) in equation (15), which can be solved to yield the finite radial extent of the pump DW in k_r space, and, equivalently, localization in real space with a typical scale length $\propto \sqrt{L_* \rho_i}$. We note that this localized mode structure due to nonuniform $\omega_*(r)$ corresponds to the finite radial envelope L_P discussed in the previous section.

As $k_r \to \infty$, the dominant term in the potential well of equation (15) is the DW kinetic dispersiveness term (the term proportional to $C_d \rho_i^2 k_r^2$); thus, it yields a bounded solution in Fourier space. If the nonlinear drive is strong enough, with $|\omega^2 - \omega_G^2| \simeq |2\gamma\omega_G| \gg |C_G \omega_G^2 \rho_i^2 k_r^2|$, the KGAM kinetic dispersiveness term can be ignored. As a result, the KGAM excitation will reduce to the GAM excitation limit; i.e.,

$$\left(\frac{\omega_*}{L_*^2}\frac{\partial^2}{\partial k_r^2} + \omega - \omega_P + \omega_* - C_d \omega_* \rho_i^2 k_r^2 + \frac{\omega k_r^2 \Gamma_0^2}{\omega^2 - \omega_G^2}\right) A_S = 0. \tag{16}$$

The reduced nonlinear DW sideband eigenmode equation in Fourier space, equation (16), yields the following dispersion relation

$$\frac{L_*^2}{\omega_*}(\omega - \omega_P + \omega_*)\beta^2 = 2l + 1, l = 0, 1, 2, 3 \cdots \tag{17}$$

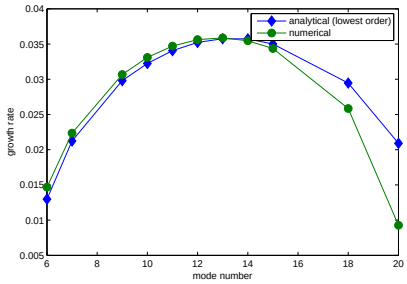

FIG. 2: Growth rates of parametric instability for different radial eigenmode numbers. Here, the circles represent the numerical solution of equation (15) while diamonds represent the analytical solution given by equation (17)

with β given by

$$\beta^4 \frac{L_*^2}{\omega_*}\left(C_d\omega_*\rho_i^2 + \frac{\omega\Gamma_0^2}{\omega_G^2-\omega^2}\right) = 1.$$

The eigenmode structure of DW sideband in Fourier space is given by

$$A_S \propto \exp\left(-\frac{k_r^2}{2\beta^2}\right), \tag{18}$$

with an extent of $|k_r| \simeq |\beta|$. A posteriori, this is also consistent with our assumption that the DW sideband eigenmode must be localized in Fourier space to satisfy the $|C_G\omega_G^2\rho_i^2k_r^2| \ll |\omega^2-\omega_G^2| \simeq |2\gamma\omega_G|$ condition.

The comparison of the analytical solution, equation (17), with the numerical solution of equation (15) is shown in Fig. 2. For most unstable mode with moderate radial eigenmode number, the analytical solution of the reduced eigenmode equation shows a quite good accuracy compared with the numerical solution of the full eigenmode equation. The nonlinear eigenmode structure is also shown in Fig. 3, which is localized in Fourier space as we expected. Thus, our assumption of ignoring kinetic dispersiveness of KGAM is self-consistent.

In Sec. IV, the coupled nonlinear equations (9) and (10) with uniform pump amplitude and ω_G have been solved numerically as an initial value problem. There, the initial perturbation is located at r_0, where the diamagnetic frequency is peaked. As a consequence, we observe that the coupled GAM and DW sideband wave packets propagate away from their original position. When the radial position of DW sideband turning points is reached, due to the nonuniform diamagnetic frequency, the wave packet will be reflected and propagate through r_0 again. Meanwhile, due to DW sideband reflection, the convective instability

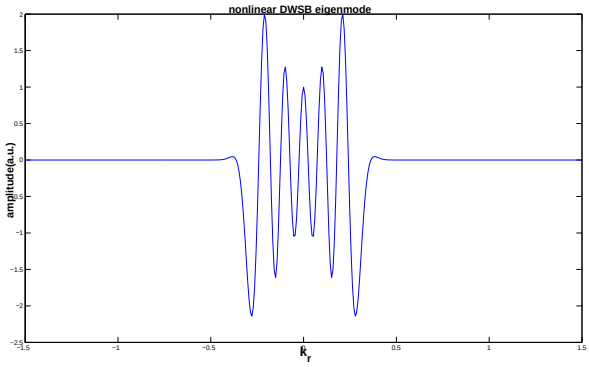

FIG. 3: Nonlinear DW eigenmode structure in Fourier-k_r space.

becomes a quasi-exponentially growing absolute instability. The GAM amplitude logarithm at r_0 is shown in Fig. 4; and we can see that the amplitude of GAM at r_0 first grow, and then decays, and then grows again. Thus, it is clearly a convective instability behavior between in time interval of $0 - 1500$ time steps, which confirms our analysis in the previous section. When one looks at longer time scale behavior, the outward propagating wave packet will, again, get to the DW turning points and be reflected. The time asymptotic behavior of the GAM amplitude at the origin, thus, becomes quasi-exponentially growing when the nonlinear eigenmode, derived analytically, is being set up.

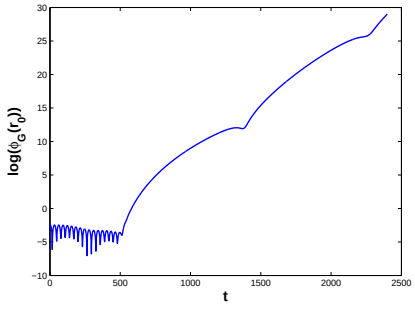

FIG. 4: GAM amplitude Logarithm at the origin v.s. time.

B. Nonuniform GAM and DW Sideband

With all the nonuniformities self-consistently included, the coupled nonlinear equations (9) and (10) must be solved numerically. Here, the pump wave is assumed to be the linear

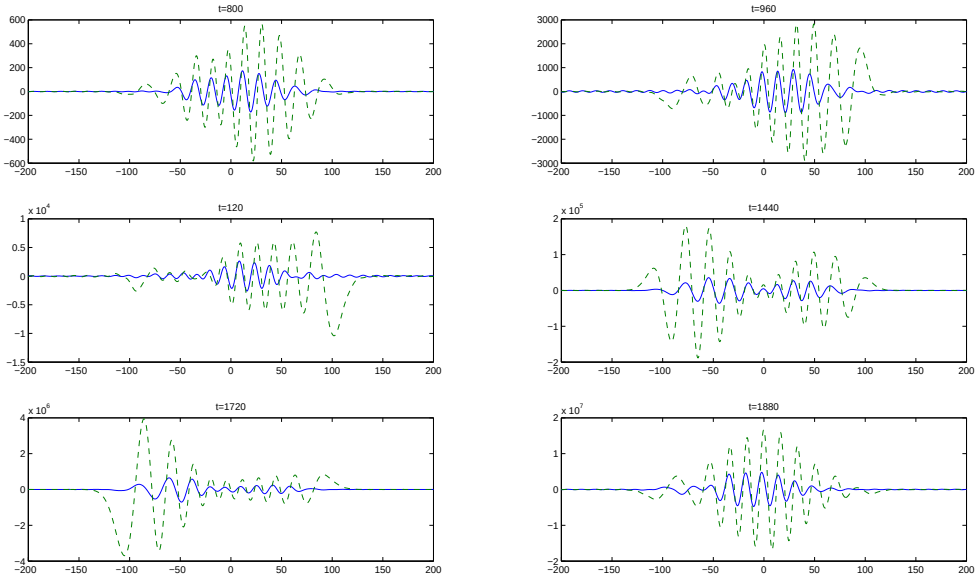

FIG. 5: Snapshots of mode structure at six different times

DW eigenmode determined by the radial profile of $\omega_*(r)$ and the DW kinetic dispersiveness, $\omega_G^2(r)$ is taken as a monotonically decreasing function of r, and $C_d = C_G = 1$ is chosen, such that the parametric instability is a convective instability on the short time scale, as we discussed in Sec. III. Due to nonuniformity of GAM continuum, one may obtain from the matching conditions that the excited KGAM has a larger k_r in the outer region of r_0 and, consequently, larger growth rate.

The mode structures of coupled DW sideband and GAM at six different times are shown in Fig. 5. One may see that, due to the nonuniformity induced by GAM continuum, the mode structures propagating on both sides are not symmetric. The wave packet initially propagating outward, has a larger k_r and, thus, larger growth rate and group velocity. Consequently, one may observe that, it also has a larger amplitude; then it is reflected at the turning point induced by $\omega_*(r)$, and propagates inward, completing a full "bouncing" period of wave packets radially trapped by nonuniform ω_*.

Time histories of GAM amplitude at $r = r_0$ is shown in Fig. 6, in which the solid curve corresponds to the nonuniform GAM frequency case, while the dashed line, illustrates the uniform GAM frequency case for comparison. One may see that, both cases are qualitatively similar; i.e., the nonuniformity of $\omega_*(r)$ is the dominant effect on the longer time scale, which

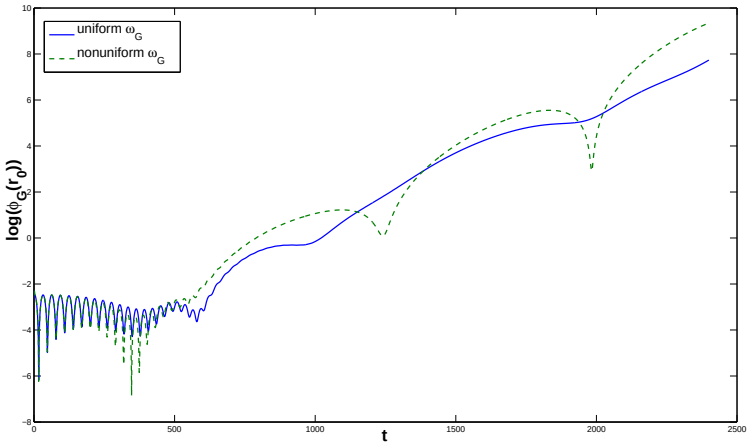

FIG. 6: Logarithm of $\mathscr{E}(r_0)$ v.s. t. Here, we take a localized pump, and nonuniform $\omega_*(r)$, and the solid curve represents the result with nonuniform $\omega_G(r)$, while the dashed curve represents the result with uniform ω_G

renders the convective parametric instability into a quasi-exponentially growing absolute instability. We may also see that, from the comparison between uniform and nonuniform $\omega_G(r)$ cases on may conclude, that GAM continuum plays a relatively minor role here, compared with $\omega_*(r)$. Due to the mismatches [26] induced by spatially varying $\omega_G(r)$, the case with nonuniform $\omega_G(r)$ has a slightly smaller growth rate, since GAM frequency change is small in the localization domain of the DW pump. For comparison, in Fig. 7, we show another case, with nonuniform $\omega_G(r)$ and $\omega_*(r)$, but uniform pump amplitude. We may see that, the qualitative behavior is the same as that of a localized pump, but the growth rate is larger here due to the larger period of parametric amplification. However, a more careful comparison of numerical results in Figs. 5 and 6, suggests that significant effect of nonuniform $\omega_G(r)$ is present on time scales comparable or shorter than the DW trapped time due to nonuniform $\omega_*(r)$. Experimentally, such effect should be measurable with sufficient spatial (radial) and temporal resolution to sample DW and GAM radial profiles after an impulsive excitation of DW turbulence burst.

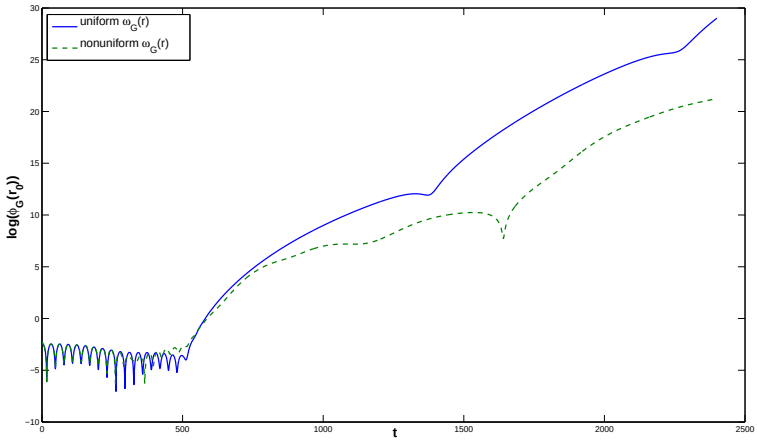

FIG. 7: Logarithm of $\mathscr{E}(r_0)$ v.s. t. Here, we take a uniform pump, and nonuniform $\omega_*(r)$, and the solid curve represents the result with uniform $\omega_G(r)$, while the dashed curve represents the result with nonuniform ω_G

V. CONCLUSIONS AND DISCUSSIONS

In this paper, spontaneous excitation of GAM by DW turbulence, which is generally accepted to be important in regulating DW turbulence, is investigated taking into account the effects of nonuniformities and finite group velocities of DW and GAM due to kinetic dispersiveness. There are three different spatial scales in the parametric instability processes between GAM and DW turbulence; i.e., DW radial envelope scale length L_P, diamagnetic frequency $\omega_*(r)$ radial profile L_*, and GAM continuum L_G, with $L_P \sim \sqrt{L_*\rho_i} \ll L_*, L_G \sim a$. In this paper, the effects of various nonuniformities on GAM nonlinear excitation are discussed, with emphasis on the convective/absolute nature of the parametric instability [26].

For typical tokamak parameters, GAM and DW sideband satisfying the wavenumber matching conditions propagate in the same direction [7, 24], and, thus, the parametric decay process of DW into GAM is a convective instability. When one considers finite radial envelope of the pump DW and the finite linear group velocities of GAM and DW sideband, the excited GAM and DW sideband are coupled and propagate out of the unstable domain in a time scale of order L_P/V_C, with $V_C \simeq V_d/2$. Here, V_d is the linear DW group velocity, such that this time is comparable with that for DW linear eigenmode set up. Thus, one

needs to consider the diamagnetic drift frequency $\omega_*(r)$ radial profile. Due to the turning points induced by ω_* nonuniformity, DW sideband and, thus, GAM, are reflected; propagating between the turning points and rendering time asymptotically the parametric decay process into a quasi-exponentially growing absolute instability. The effect of nonuniform $\omega_*(r)$ on GAM excitation is also investigated analytically for a strong drive case, when the finite dispersiveness of GAM can be neglected. Lastly, the self-consistent problem including all three nonuniformities is investigated numerically, and our results indicate that the radial profile of $\omega_*(r)$ plays the dominant role in rendering the convective instability into a quasi-exponentially growing absolute instability. The nonuniformity of GAM continuum, meanwhile, introduces asymmetries between outward and inward propagating modes, but the qualitative picture remains the same. Our results, thus, indicate that, to properly interpret the experimental results of GAM excitation by DW turbulences, plasma nonuniformities must be taken into considerations; which could change the properties of the parametric process qualitatively.

A major assumption of this work is that the amplitude of the sideband is much smaller than that of the pump DW, $A_S \ll A_0$, and, hence , we separate $\phi_d = \phi_P + \phi_S$. This assumption, often applied to derive the growth rate and threshold condition, is applicable only in the linear growth stage of the parametric decay process. The feedback of the daughter waves on the pump wave, and thus, the nonlinear evolution of the turbulence spectrum, is beyond the scope intended here. To systematically study the nonlinear regulation of DW turbulence by GAM, and, consequently, DW turbulence radial spreading via excitation of GAM, a set of fully nonlinear two field model equations [28] must be derived. This will be reported in a future publication.

Acknowledgments

This work is supported by the Euratom Communities under the contract of Association between EURATOM/ENEA, USDoE GRANTS, the ITER-CN under Grants No. 2013GB104004 and No. 2011GB105001, the National Science Foundation of China under grant No. 11205132 and Fundamental Research Fund for Chinese Central Universities.

References

[1] W. Horton, Rev. Mod. Phys. **71**, 735 (1999).

[2] Z. Lin, T. S. Hahm, W. W. Lee, W. M. Tang, and P. H. Diamond, Phys. Rev. Lett. **83**, 3645 (1999).

[3] A. Hasegawa, C. G. Maclennan, and Y. Kodama, Physics of Fluids **22**, 2122 (1979).

[4] M. N. Rosenbluth and F. L. Hinton, Phys. Rev. Lett. **80**, 724 (1998).

[5] P. H. Diamond, S.-I. Itoh, K. Itoh, and T. S. Hahm, Plasma Physics and Controlled Fusion **47**, R35 (2005).

[6] N. Winsor, J. L. Johnson, and J. M. Dawson, Physics of Fluids **11**, 2448 (1968).

[7] F. Zonca and L. Chen, Europhys. Lett. **83**, 35001 (2008).

[8] Z. Lin, T. S. Hahm, W. W. Lee, W. M. Tang, and W. R. B., Science **281**, 1835 (1998).

[9] L. Chen, Z. Lin, and R. White, Physics of Plasmas **7**, 3129 (2000).

[10] R. Sagdeev and A. Galeev., *Nonlinear plasma theory* (AW Benjamin Inc., 1969).

[11] P. K. Kaw and J. M. Dawson, Physics of Fluids **12**, 2586 (1969).

[12] P. N. Guzdar, N. Chakrabarti, R. Singh, and P. K. Kaw, Plasma Physics and Controlled Fusion **50**, 025006 (2008).

[13] N. Chakrabarti, P. N. Guzdar, R. G. Kleva, V. Naulin, J. J. Rasmussen, and P. K. Kaw, Physics of Plasmas **15**, 112310 (2008).

[14] P. N. Guzdar, R. G. Kleva, N. Chakrabarti, V. Naulin, J. J. Rasmussen, P. K. Kaw, and R. Singh, Physics of Plasmas **16**, 052514 (2009).

[15] R. Hager and K. Hallatschek, Physics of Plasmas **19**, 082315 (2012).

[16] R. Hager and K. Hallatschek, Phys. Rev. Lett. **108**, 035004 (2012).

[17] N. Chakrabarti, R. Singh, P. K. Kaw, and P. N. Guzdar, Physics of Plasmas **14**, 052308 (2007).

[18] J. Yu, J. Dong, X. X. LI, D. Du, and X. Y. Gong, Journal of Plasma Physics **78**, 651 (2012).

[19] J. Yu and J. Dong, Physica Scripta **82**, 045504 (2010).

[20] Z. Lin, S. Ethier, T. S. Hahm, and W. M. Tang, Phys. Rev. Lett. **88**, 195004 (2002).

[21] F. Zonca, R. B. White, and L. Chen, Physics of Plasmas **11**, 2488 (2004).

[22] E. A. Frieman and L. Chen, Physics of Fluids **25**, 502 (1982).

[23] Z. Qiu, L. Chen, and F. Zonca, Plasma Physics and Controlled Fusion **51**, 012001 (2009).

[24] L. Chen, F. Zonca, and Z. Qiu (Varenna, Italy, 2010).

[25] D. Kong, A. Liu, T. Lan, Z. Qiu, H. Zhao, H. Sheng, C. Yu, L. Chen, G. Xu, W. Zhang, et al., Nuclear Fusion **53**, 113008 (2013).

[26] M. N. Rosenbluth, Phys. Rev. Lett. **29**, 565 (1972).

[27] Z. Qiu, F. Zonca, and L. Chen, Physics of Plasmas **19**, 082507 (2012).

[28] Z. Guo, L. Chen, and F. Zonca, Phys. Rev. Lett. **103**, 055002 (2009).